Korean J. Chem. Eng., 33(12), 3425-3433 (2016)
DOI: 10.1007/s11814-016-0222-3

pISSN: 0256-1115
eISSN: 1975-7220

Polycyclic aromatic hydrocarbon emissions of non-road diesel engine treated with non-thermal plasma technology

Jianbing Gao*, Chaochen Ma*,†, Shikai Xing, Liwei Sun*, and Jiangquan Liu***

*School of Mechanical Engineering, Beijing Institute of Technology, Beijing 100081, China
**School of Vocational and Technical, Hebei Normal University, Shijiazhuang 050024, China
(*Received 22 May 2016 • accepted 1 August 2016*)

Abstract−Non-road diesel engines are important polycyclic aromatic hydrocarbon (PAH) sources in the environment due to their high emission concentration compared to on-road diesel engines. Particle- and gas-phase PAH concentrations of a non-road diesel engine were investigated. Non-thermal plasma (NTP) as an effective after-treatment technology was used to reduce PAH emissions. The results showed that particle-phase PAH concentrations were 329.7 μg/m^3, 3,206.7 μg/m^3, and 1,185.7 μg/m^3 without the action of NTP at three different engine loads respectively. Relatively low concentrations were measured for gas-phase PAHs. Excellent linearity was shown for particle-phase with total PAH concentrations both with, and without, NTP. The gas-phase PAH concentrations linearly increased with engine load without NTP. The five most abundant compounds of PAHs were among low molecular weight (LMW) and medium molecular weight (MMW) compounds. Total PAH cleaning efficiency was beyond 50% when treated with NTP at the three different engine loads. We hypothesized that naphthalene (Nap) concentrations increased greatly at 60% and 80% engine loads because it was produced within the plasma zone by decomposition of high molecular weight (HMW) PAHs. The PAHs content of particulate matter (PM) aggregation at 60% load was approximately three times higher than at 40% and 80% loads. High correlation values were observed for MMW PAHs with total PAH concentrations. Correlations of PAH concentration reduction could be important to clarify the PAH reduction mechanism with NTP technology.

Keywords: Diesel Engine, Non-thermal Plasma, Polycyclic Aromatic Hydrocarbon, Phase Distribution

INTRODUCTION

Cancer incidence rates have increased in recent years [1,2] and PAHs are seriously carcinogenic, teratogenic, and mutagenic pollutants [3], being one of the reasons for the increase in cancer incidence. The World Health Organization recommends that benzo[a]pyrene annual mean concentrations should not exceed 1 ng/m^3; however, the concentrations thereof in many cities exceed this [4]. Engine exhausts are the primary source of PAH emissions [5,6], which is also demonstrated by the sudden drop of PAH concentrations of Londrina on Sunday due to the reduced number of diesel buses running [6]. About 80% of PAH emissions come from diesel vehicles in Australia [7].

The main sources of diesel PAH emissions are pyrolysis products from fuel combustion, and their survival in diesel fuel and lubricating oil [7]. Biodiesel fuels are used to reduce exhaust emissions [8-11]; however, the removal efficiency of PAHs is less than 20%, as found by He [8]. Diesel particle filters (DPF) are the most successful PM removal after-treatment technology and HMW PAHs are easily cleaned by DPF, while data are inconsistent for LMW PAHs [12]. As an alternative diesel engine exhaust after-treatment technology, NTP allows simultaneous removal of hydrocarbons (HC), nitrous oxides (NO_x), and PM [13-16]. Removal of PM and HC means that particle- and gas-phase PAHs can also be removed effectively.

An abundance of active ions is found in the plasma zone when a high voltage is applied to an NTP reactor. PAHs are partly oxidized into CO_2 and H_2O or breakup into LMW PAHs under the effect of active ions, which effectively reduces PAH emissions. Some particle-phase PAHs can be captured on the collection plate of the NTP reactor when engine exhaust flows through it. The conversion of NO to NO_2 with the assistance of plasma is conducive to HC oxidation (including PAHs). Emission concentrations of non-road diesel engines are several times higher than that of road diesel engines due to their poor combustion and lack of after-treatment technology, and they cause more environmental and health problems [17]. Xu [18] studied the decomposition effect of NTP on PAHs; the efficiency reached 80% when the applied voltage was 40 kV. The PAHs were generated by garbage incineration, and the NTP reactor was designed based on the pulse corona discharge. The effect of direct NTP technology on PAH emissions of diesel engine was researched [19]; the PAH concentration decreased and then increased with increasing engine load. While the PAH removal efficiency was low, that the value was 40.48%. Cai [20] reduced the PAH emissions emitted by a diesel engine using NTP technology; the results showed that the maximum removal efficiency was 37.87%. And the analysis of the PAHs both in particle- and gas-phase was performed together. Similar work reducing the PAH emissions using

†To whom correspondence should be addressed.
E-mail: machaochen1900@163.com

NTP technology was also done by Du [21], with the removal efficiency of PAHs ranging from 70.3% up to 74.4%. The mechanism of PAH reduction using NTP technology was mentioned as that the primary route of PAH reduction was considered to be an OH reaction with aromatic rings. While, some PAHs can be oxidized by the active ions in the plasma zone directly. To deduce the reduction mechanism of PAHs, four PAHs as the targets were treated using gliding arc discharge [22]. It was pointed out that the energetic electron and active radicals generated in the plasma played a vital role in PAH reduction. Many countries have enacted emission standards to restrict non-road diesel engine emissions; however, they do not cover for diesel engines of less than 8 kW power output in Europe, Japan, and China. Little work has been done to investigate PAH emission concentrations of low power non-road diesel engines (<8 kW) and measurements to reduce their PAHs emissions.

In this work, we investigated PAH distributions of a low power non-road diesel engine at different engine loads both with, and without, NTP. An NTP reactor was designed based on the corona discharge principle to decrease PAH concentrations. Both particle- and gas-phase PAHs were taken into account. The correlation analysis of PAH emission concentrations of a non-road diesel engine was also investigated.

MATERIAL AND SECTION

1. Test Diesel Engine

A small-displacement diesel as a daily-used diesel power generator was used to characterize the PAH emissions. Technical specifications of the diesel engine generator are listed in Table 1. This type of diesel generator is normally used in large quantities in many regions of China. The diesel generator had run for less than 100 hours.

Table 1. Technical specifications of the diesel generator

	Items	Parameters
Engine	Manufacturer	KEPU
	Engine type	KD186FA
	Number of cylinders	Single
	Displacement	0.418 L
	Compression ratio	19
	Injection pressure	21 MPa
	after-treatment system	Without
	Speed	3000 rpm
Generator	Voltage	220 V
	Rated power	5.0 kW

2. PAH Sampling

The sampling temperature should be below 52 °C, and the particle-phase PAHs were defined as the PAHs collected on a filter at a temperature of 52 °C (or less) [23]. Both particle- and gas-phase PAHs were sampled using a PAH collection system (Fig. 1). Particle- and gas-phase PAHs were collected using glass fiber filter paper (Whatman GF/A55) and self-made "PUF/XAD-2/PUF" at 35 °C, respectively. Glass fiber filter papers were baked for 6 hours at 400 °C in a muffle furnace before sampling. Details of PUF/XAD-2/PUF are given in the State Environmental Protection Standards of the People's Republic of China: HJ 646-2013. Particle- and gas-phase PAHs were sampled at 10 L/min exhaust flow rate for 10 min, and PM aggregation was undertaken at 200 L/min over dozens of minutes. Samples were wrapped with aluminum foil and stored in a refrigerator at below 4 °C after sampling. A vacuum pump was installed downstream of the flow meter to extract the exhaust gas.

The temperature of the NTP reactor was about 150 °C, and the applied voltage (direct current) was −7,000 V. The taper angle of

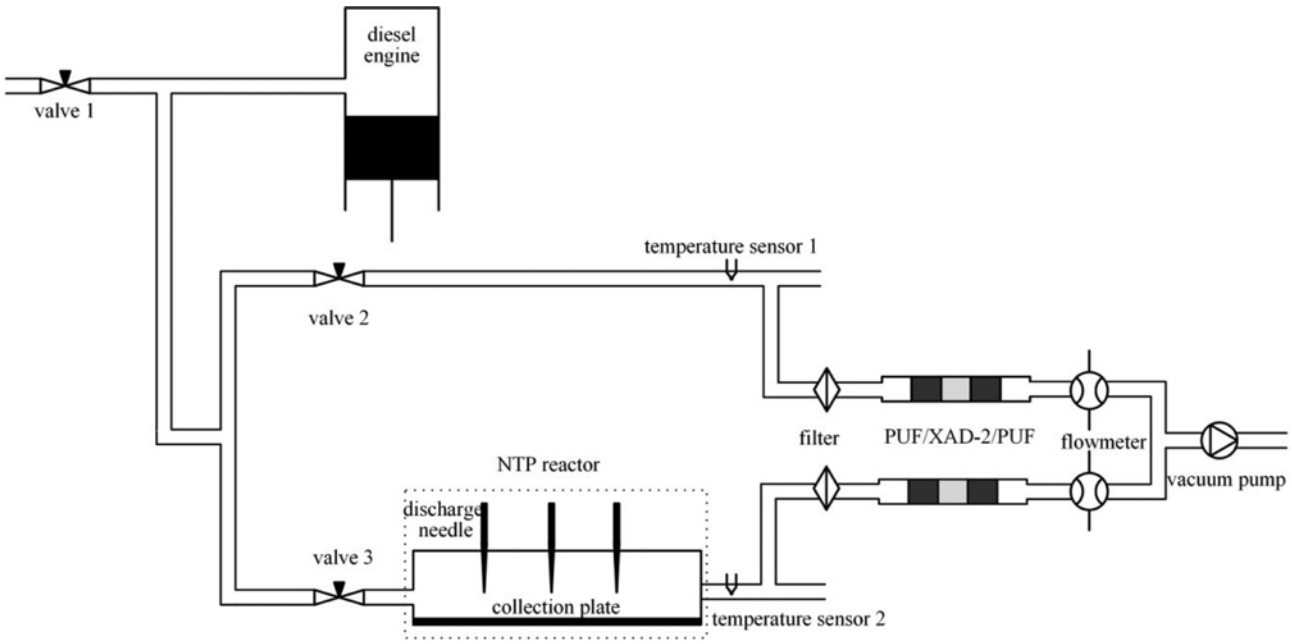

Fig. 1. PAH sampling scheme.

Table 2. Sampling conditions

Sample	Engine load/%	NTP condition	PAH phase
1	40	With	Particle-phase
2	40	With	Gas-phase
3	40	With	PM aggregation
4	40	Without	Particle-phase
5	40	Without	Gas-phase
6	60	With	Particle-phase
7	60	With	Gas-phase
8	60	With	PM aggregation
9	60	Without	Particle-phase
10	60	Without	Gas-phase
11	80	With	Particle-phase
12	80	With	Gas-phase
13	80	With	PM aggregation
14	80	Without	Particle-phase
15	80	Without	Gas-phase

the discharge needle was 30°, and the distance between discharge needle and the collection plate was 10 mm. The 16 discharge needles were uniformly distributed on the area (0.18 m×0.23 m) of NTP reactor. High voltage direct current was applied to the discharge needle, and the collection plate was connected to the ground. The voltage was supplied by a high voltage DC power supply. Part of the PM in the exhaust was collected on the collection plate (PM aggregation), which was then peeled off from the collection plate to investigate its PAH content. Regeneration of NTP reactor (corona discharge, dotted line, Fig. 1) involves the PM aggregation oxidation, which could cause secondary PAH emissions. It is also necessary to clarify the PAH characteristics of PM aggregation.

3. Measurement Protocol

The speed of the diesel engine was constant. Engine loads could be controlled by electrical power outputs of a generator. PAH content of particle-, gas-phase, and PM aggregation was investigated at different engine loads (Table 2).

4. PAH Extraction and Analysis

Particle- and gas-phase PAHs were extracted from glass fiber filter paper and PUF/XAD-2/PUF, respectively, by using an accelerated solvent extraction system (Dionex ASE 200), and the extraction conditions were as follows: mixed solvent (acetone : n-hexane, 1 : 1), pressure (1,500 psi (10.34 MPa)), temperature (100 °C), pre-heating time (2 min), cycle index (3). The extracts were concentrated in a rotary evaporator to 1 mL then stored below 4 °C.

Qualitative and quantitative analysis of PAHs were performed using a gas chromatograph-mass spectrometer (GC-MS, Agilent 7890A/5975C) under selected ion monitoring (SIM) scanning. The GC-MS was equipped with a capillary column (HP-5, 30 m×250 μm×0.25 μm) with an injection volume (1 μL) and delay time (5 min). The splitless injection and ion source temperatures were 280 and 230 °C, respectively. The oven temperature was held at 70 °C for 2 min and programmed to increase to 280 °C at 10 °C/min (held for 5 min), and then to 300 °C at 5 °C/min (held for 5min). Relative standard deviation (RSD), limits of detection and recoveries of 16 PAHs were 0.5%-10.1%, 0.03 mg/L-0.67 mg/L and 55.78%-103.46%, respectively. Details of the limits of detection, RSD, and recoveries are listed in Table S1.

The 16 quantified PAHs are classified by molecular weight. Low molecular weight (LMW): Naphthalene (Nap), Acenaphthylene (AcPy), Acenaphthene (Acp), Fluorene (Flu), Phenanthrene (PA), Anthracene (Ant); medium molecular weight (MMW): Fluoranthene (FL), Pyrene (Pyr), Benzo[a]anthracene (BaA), Chrysene (CHR). High molecular weight (HMW): Benzo[b]Fluoranthene (BbF), Benzo[k]Fluoranthene (BkF), Benzo[aPyrene (BaP), Indeno [1,2,3-cd]Pyrene (IND), Dibenzo[a,h]Anthracene (DBA), and Benzo [g,h,i]Perylene (BghiP) [24].

RESULTS AND DISCUSSION

PAHs emitted from diesel engines were in particle- and gas-phase, and their distributions mainly depended on vapor pressure

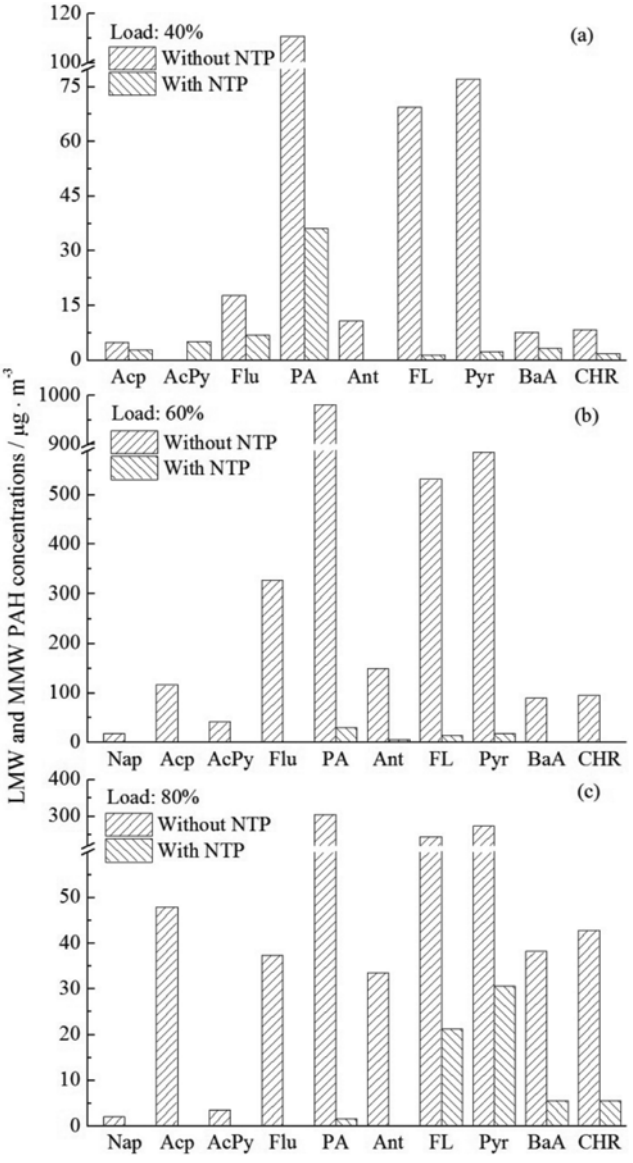

Fig. 2. Particle-phase LMW and MMW PAH concentrations at (a) 40%, (b) 60%, (c) 80% engine load.

and temperature [23]. The sampling temperature of the PAHs samples was 35 °C. LMW (2- and 3-rings) PAHs are mainly in the gas-phase and they are primarily particle-phase for HMW (5- and 6-rings) PAHs. Toxicity factors of HMW PAHs are higher than LMW PAHs (Table S1) that HMW PAHs do more harm to human health and environment. The effects of engine loads on total PAH emissions are inconsistent in that the total PAH emissions are almost the same for a bus using with ultralow-sulfur diesel fuels; however, they are doubled at 50% load compared with 25% load when using low-sulfur diesel fuels [7]. No matter the engine work conditions, LMW PAHs predominate in PAH emissions, as shown in the literature [3-5,25-28].

1. Particle-phase PAH Emissions

Considering the concentration differences of individual PAHs, the PAH concentrations were shown separately. Figs. 2(a)-(c) show particle-phase LMW and MMW PAH concentrations at 40%, 60%, and 80% engine loads, respectively. The RSDs (error bars) are shown in Table S1. Higher PAH concentrations were observed at 60% load than at 40% and 80% without NTP, which disagreed with some results in that particle-phase PAHs decreased with engine load [24]. Richer fuel/air mixtures (higher engine load) led to more PAH emissions, while the richer mixture also meant a higher combustion temperature making PAHs easier to oxidize.

Nap, and AcPy concentrations were low at the three different engine loads for particle-phases without an NTP reactor (Lou [29] indicated the same tendency). PA, FL, and Pyr were in the majority, no matter the engine load. Concentrations of these three PAHs of 60%, 80% load were dozens of times more than some road diesel engines [4,28,30], because of the poor combustion and no after-treatment technology for non-road diesel engine (<8 kW) without the restriction of emission regulations. PAH emission concentrations from the non-road diesel engine were similar with those of an old bus powered by an engine made in 1975 [4]. The results indicated that huge amounts of PAHs were emitted by non-road diesel engine so that stringent emission regulations should be enacted. LMW and MMW PAHs, except Acpy at 40% load, decreased sharply because of the NTP, and the emission concentrations were similar to those from road diesel engines [4]. This decrease of PAH emissions was attributed to several reasons, such as electrostatic precipitation, partial oxidation of PAH, and polymerization. FL, Pyr predominated in the emissions of LMW and MMW PAHs at 80% engine load with the effect of the NTP while PA and Flu prevailed at 40% engine load.

Because HMW PAHs condense on PM and tend to be more toxic, study of the particle-phase HMW PAHs was crucial. Particle-phase HMW PAH concentrations at different engine loads are shown in Figs. 3(a)-(c). Concentrations of HMW PAH were lower than LMW and MWM PAHs and the concentration was the lowest at 40% load, and highest at 60%. Particle-phase BbF concentrations were 81.3 μg/m^3 and 45.1 μg/m^3 at 60% and 80% load, respectively. BghiP was greater than 35 μg/m^3 at 80% load, while it was less than 6.5 μg/m^3 at 40% and 60% load.

The HMW PAH concentrations were highest at 80% load with the NTP, although they were lower than at 60% load without the NTP. Higher combustion temperatures lowered the surface activity of PM and lead to PM graphitization rates, which made PM

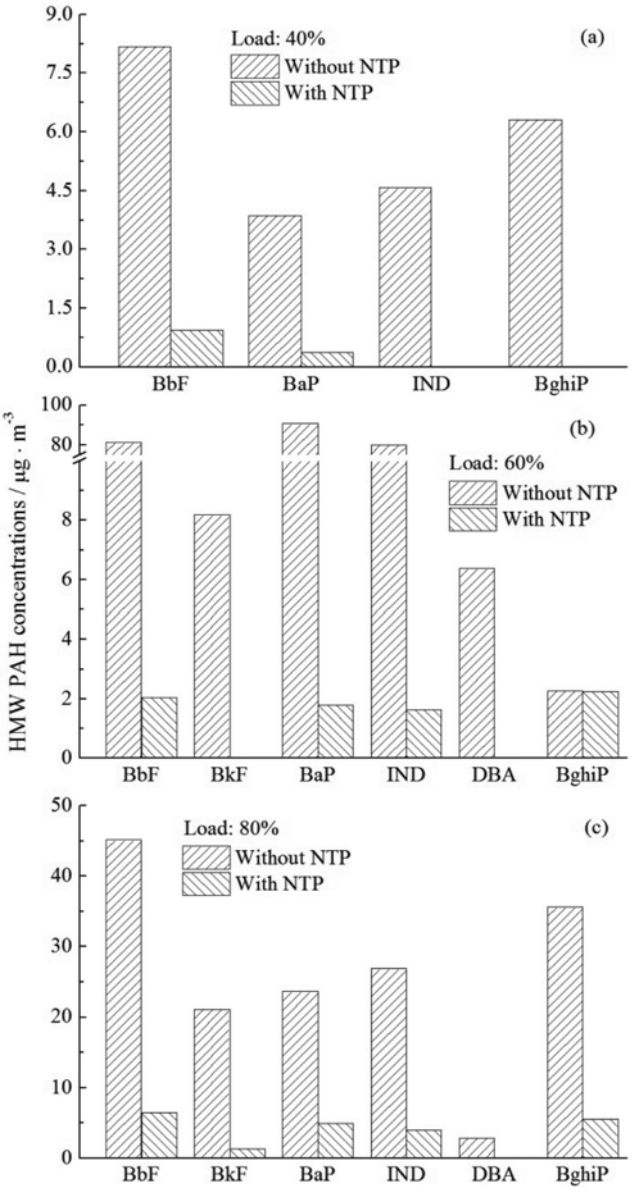

Fig. 3. Particle-phase HMW PAH concentrations at (a) 40%, (b) 60%, (c) 80% engine load.

oxidation more difficult [31]. Some PAHs concentrations dropped to zero when treated with NTP. The highest contributors for HMW with NTP were highly toxic BbF (6.4 μg/m^3) and BaP (5.0 μg/m^3) at 80% load. Large reduction of HMW PAH concentrations led to a substantial drop in PAH toxicity.

Particle-phase PAH concentrations decreased greatly under the influence of NTP. Two reasons caused this PAH reduction: (1) part of the particle-phase PAHs are captured on the collection plate. The maximum PM removal efficiency (capture and oxidation) reaches 76.9% at −5,000 V and it increases with voltage [32]. Part of the NO in engine exhaust is oxidized into NO_2 [33,34], which is conducive to PM oxidation [35]. A higher PM removal efficiency means higher particle-phase PAH removal performance. (2) Under the action of the plasma, part of the MMW and HMW particle-phase PAHs decayed to CO_2 or LMW PAHs (these may have been

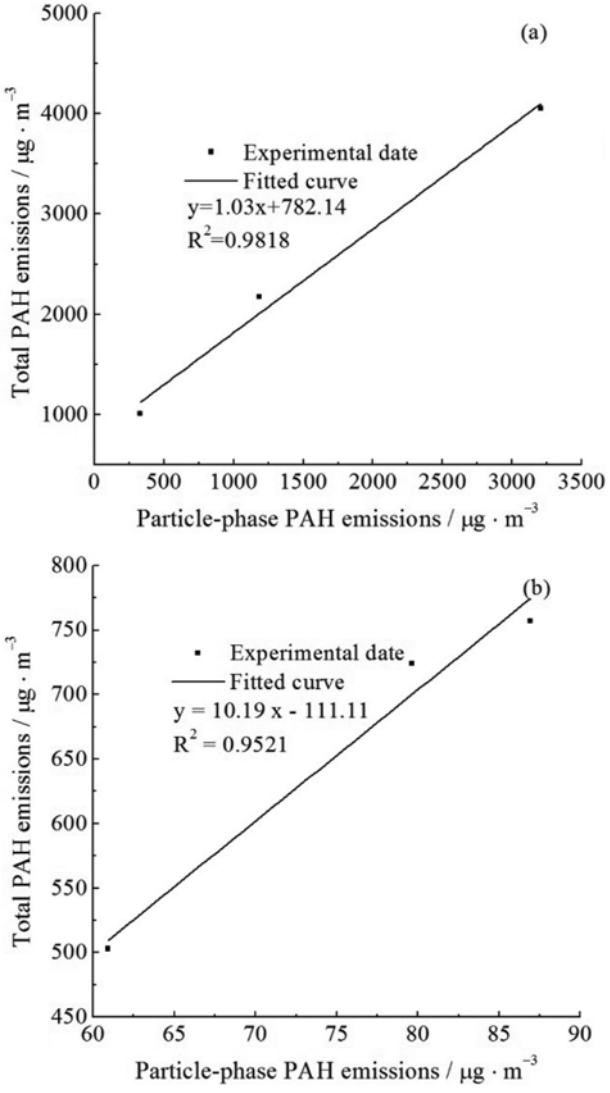

Fig. 4. Correlation analysis of PAH emissions (a) without (b) with, NTP.

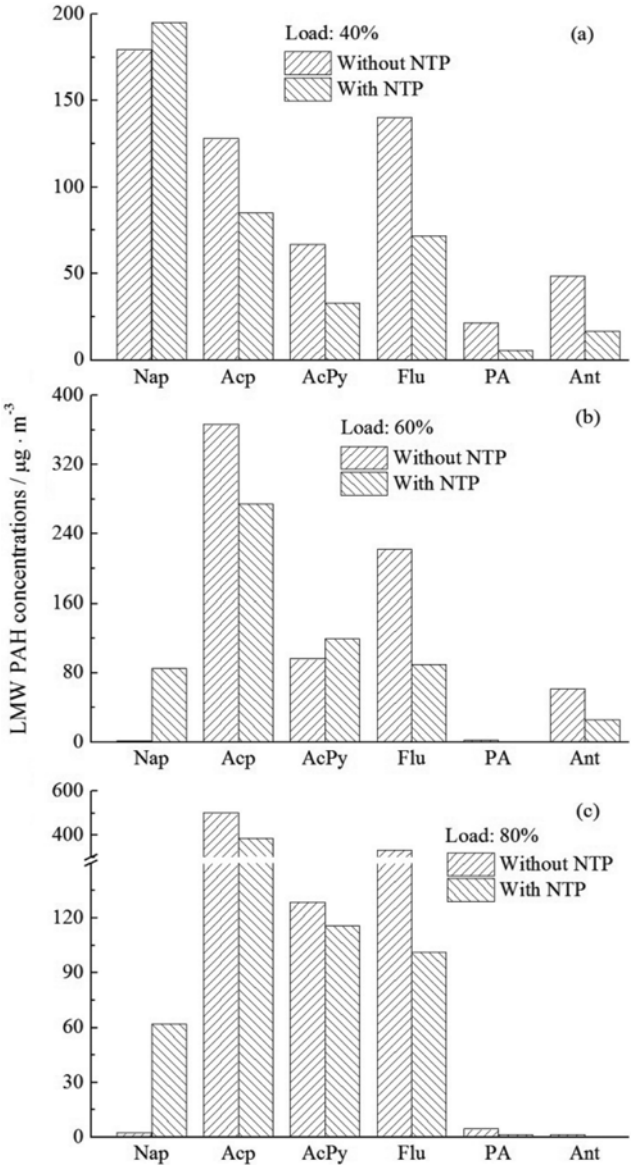

Fig. 5. Gas-phase LMW PAH concentrations at (a) 40%, (b) 60%, (c) 80% engine load.

present in the gas-phase due to their high vapor pressure).

The particle-phase concentration was almost linearly correlated with total PAH concentration both with, and without NTP (Fig. 4). Particle-phase PAHs were predominant in total PAHs without NTP; however, it was *c.* 10% with NTP. He [8] finds correlation coefficients of raw PAH concentrations were 0.9735, 0.7106, and 0.8867 for engines fuelled with diesel, biodiesel 20 (20% biodiesel blended with 80% diesel), and pure biodiesel.

2. Gas-phase PAH Emissions

Quantities of unburned fuel and pyrolysis products cannot be completely oxidized in the engine exhaust and are present in the gas-phase. Figs. 5(a)-(c) show gas-phase LMW PAH concentrations at 40%, 60%, and 80% engine loads. Nap concentration of the diesel exhaust at 60% and 80% loads was lower than many other PAHs, while it predominated the PAH concentrations in other studies [4,8,26]. Acp, AcPy, and Flu were the highest contributors to LMW PAHs at 60% and 80% load, while these were Nap, Acp, AcPy, and Flu at 40% load. The reduction performance for LMW gas-phase PAHs differed from that of the particle-phase in that the Nap concentration increased rapidly for the breakup of MMW and HMW PAHs. Nap concentrations were 195.1 μg/m^3, 84.8 μg/m^3, and 61.9 μg/m^3 at 40%, 60%, and 80% load with NTP, respectively.

Figs. 6(a)-(c) show gas-phase MMW and HWM PAH concentrations at different engine loads. FL concentrations were 43.6 μg/m^3 and 62.3 μg/m^3 at 40% and 60% load being 20 times higher than those at 80% load. Many PAHs were not detected, especially HMW PAHs, which some results also demonstrated that the gas-phase HMW PAHs were only present in small quantities [36]. Under the action of NTP, the concentrations of MMW and HMW PAHs in gas-phase decreased significantly.

Excellent linearity is shown in Fig. 7 for gas-phase PAH concentrations with different engine loads (R^2=0.9963) without NTP. It was speculated that the engine exhausted plenty of gas-phase PAHs

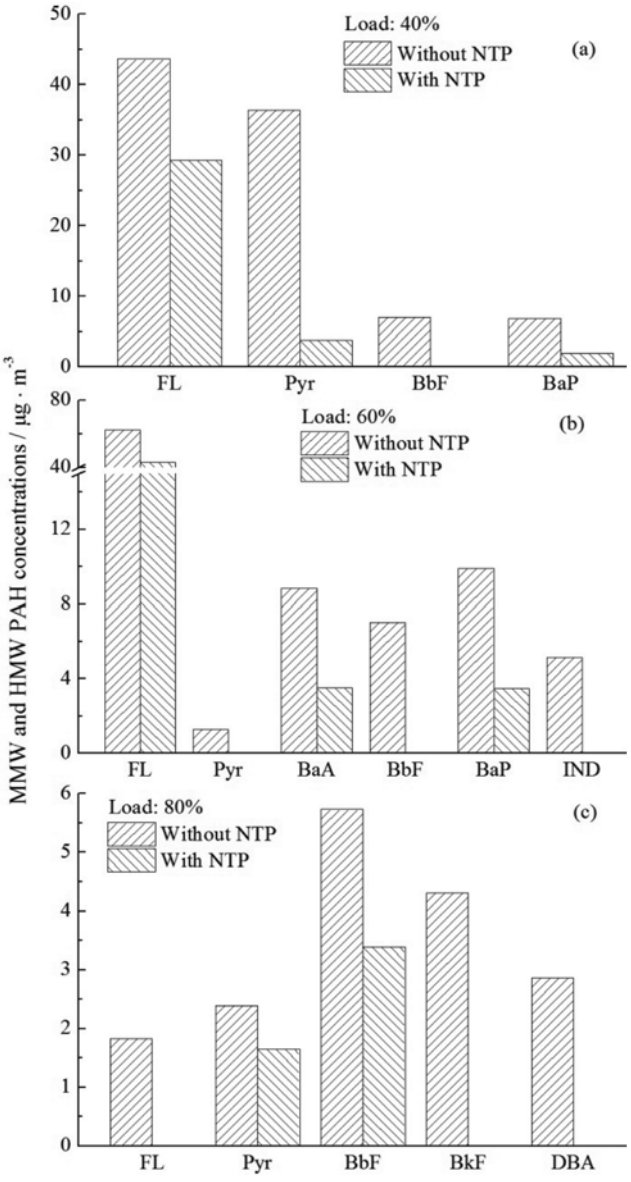

Fig. 6. Gas-phase MMW and HMW PAH concentrations at (a) 40%, (b) 60%, (c) 80% engine load.

even at no power output (*c.* 372.1 μg/m^3). Spezzano [26] investigated the gas-phase PAH emissions of non-road diesel engines and found that they were an order of magnitude more than those from road diesel engines.

PAH distributions changed greatly with the action of NTP. Table 3 lists the five most abundant compounds of total PAHs at different engine loads. Differing from other PAHs that Nap concentration increased when treated with NTP, which was caused by the breakup of HMW and MMW PAHs in the plasma atmosphere. In the plasma zone, PAHs collided with high-energy electron, and reacted with OH, which led to the breakup of aromatic rings. All the MMW and HMW PAHs contain the element of NaP (judged from the molecular structures) so that the breakup into NaP can happen theoretically. All LMW PAHs were included except Ant, and all HMW PAHs were excluded among the five most abundant compounds.

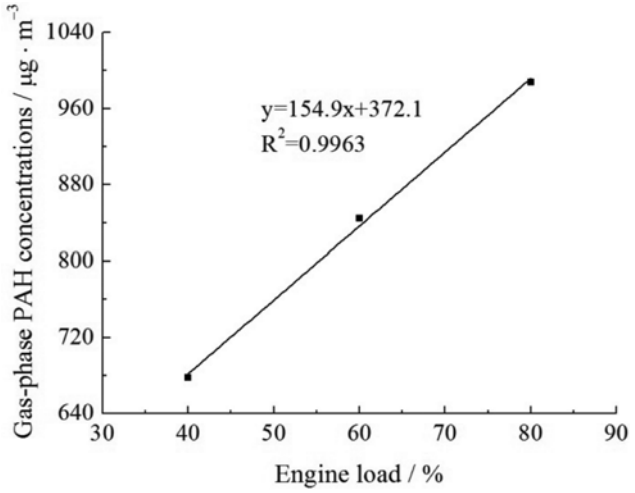

Fig. 7. Correlation analysis of gas-phase PAH concentration with engine loads.

Table 3. The five most abundant compounds in total PAHs

	40% Load		60% Load		80% Load	
	Without NTP	With NTP	Without NTP	With NTP	Without NTP	With NTP
PAHs	mg/m^3					
Nap	179.3	195.1	-	84.8	-	61.9
Acp	132.8	87.7	482.8	274.8	548.9	385.1
AcPy	-	38.1	-	119.3	-	115.6
Flu	157.8	78.8	549.0	91.6	370.0	101.1
PA	132.3	41.6	983.9	-	310.3	-
FL	-	-	593.6	57.3	247.2	-
Pyr	113.4	-	587.4	-	276.4	32.3

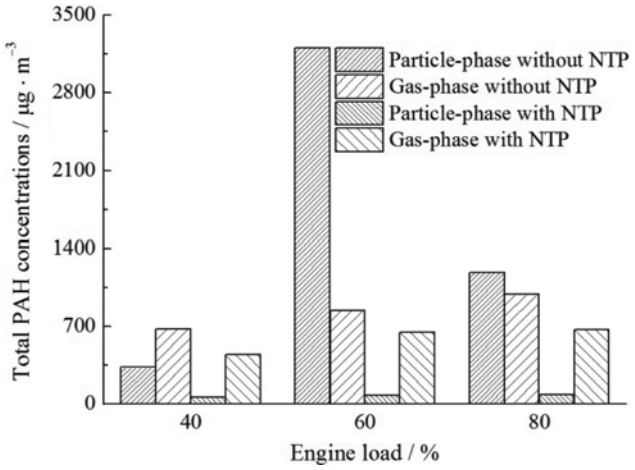

Fig. 8. Particle- and gas-phase PAH concentrations.

Additional gas-phase PAHs were added due to the breakup of MMW and HMW PAHs into LMW (maybe in the gas-phase due to their high vapor pressure) under the influence of plasma. Decomposition of HWM and MMW (particle-phase) PAHs caused

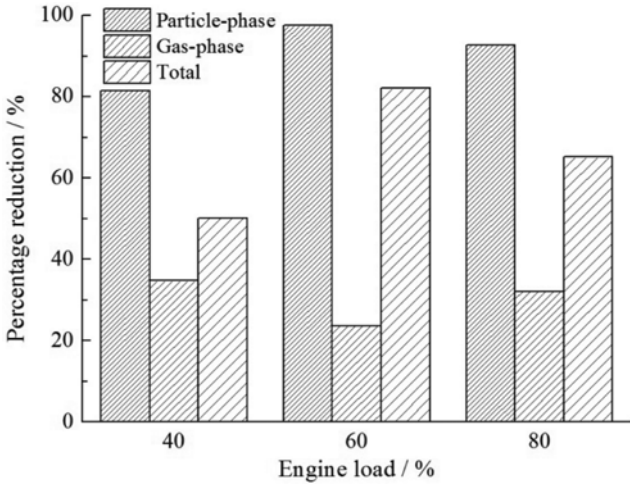

Fig. 9. Particle- and gas-phase PAH concentration percentage reduction.

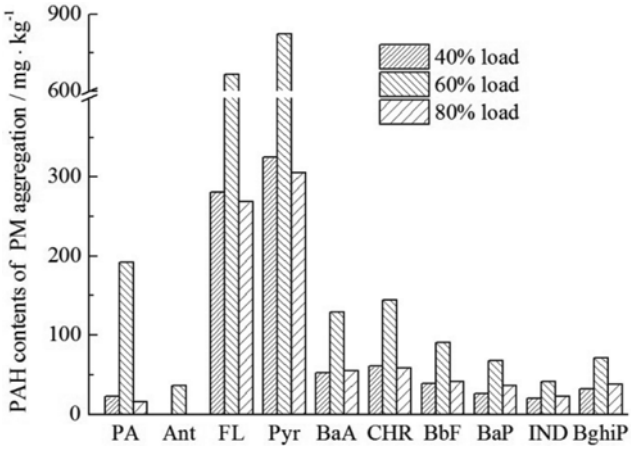

Fig. 10. PAH contents of PM aggregation.

low concentration percentage reduction for gas-phase components rather than particle-phase components (Figs. 8 and 9). The total PAH concentrations were of the same order of magnitude as found by Alkurdi [4]. The percentage reduction of total PAH concentrations was more than 50% with NTP at three different engine loads. Concentration ratios of particle- to gas-phase were almost the same (*c.* 0.13) at different engine loads with NTP. The chemical reaction mechanism of NTP and PAHs is shown as Eqs. (1)-(6). Part HC (both particle- and gas-phase PAHs) is directly oxidized into CO and CO_2 by active ions (O and O_3). The primary route of PAH reduction is thought to be a reaction with OH, as shown in Eqs. (5) and (6). Then, the ring-cleavage products of PAHs can be continuously oxidized by active ions [21]. PAHs in the plasma zone collided with high-energy electron (e^-), which also leads to the breakup of C=C and C-H.

$$HC+O \rightarrow CO_2+H_2O \quad (1)$$

$$HC+OH+2O \rightarrow CO_2+H_2O \quad (2)$$

$$HC+O_3 \rightarrow CO_2+H_2O \quad (3)$$

$$HC+NO_2 \rightarrow HCO+NO \quad (4)$$

$$OH+PAH \rightarrow OH-PAH \quad (5)$$

$$OH-PAH+O_2 \rightarrow \text{ring-cleavage products} \quad (6)$$

Compared with references [19,20], the PAH removal efficiency is high in this work that was caused by PM aggregation collected on the collection plate. That can be evidenced by the results that PM contains much particle-phase PAHs, and the removal efficiency of gas-phase PAHs is similar to the removal efficiency of total PAHs in other references [19,20]. Many countries have not enacted emission regulations for low power (<8 kW) non-road diesel engines. High PAH emissions imply that measures must be taken to reduce non-road diesel engine PAHs. The excellent particle-phase PAH removal efficiency of non-road diesel engines makes the NTP technology an alternative method of PAH removal in thermal power plants, and incinerators where many particle-phase PAHs are generated.

3. PAH Contents of PM Aggregation

Re-entrainment and the back corona phenomenon will arise with the accumulation of PM aggregation, which worsens the PM removal efficiency of NTP technology [37-39]. It is necessary to resolve these NTP regeneration problems; however, secondary PAH pollution may happen during PM aggregation oxidation, making it necessary to find the PAH content of PM aggregation (Figs. 10 and S1).

Nap, Acp, AcPy, and Flu were not detected in PM aggregation at the three different engine loads, and FL and Pyr concentrations were the highest. This was because the temperature was about 150 °C on the collection plate. For some LMW PAHs (Nap, Acp, AcPy, and Flu), they were easier to volatilize due to their high vapor pressure than MMW and HMW PAHs. The PAH content at 60% engine load (2264.6 mg/kg) was about three times higher than at 40% and 80% loads (858.2 mg/kg and 842.2 mg/kg) because the PAH content of PM aggregation was closely related to particle-phase PAH concentrations.

4. Correlations of PAHs

Table S2 shows the correlation between PAHs without NTP: these relationships can be useful to speculate on the mechanism of PAH generation during fuel combustion. Correlations of PAHs with the regulated emissions should be calculated to simplify the PAH measurement procedure [40]. High correlation values were observed for all the MMW PAHs with total PAH concentrations, which evinced the close relationship of MMW with total PAHs. The formation mechanism and generation progress of Nap, Acp and AcPy may be similar due to the high correlation values found.

Table S3 shows the correlation of PAH concentration reduction. All MMW, and some HMW, components of PAHs exhibited high correlation with total PAH concentration reduction. With the action of NTP, the breakup of MMW and HMW into LMW PAHs led to the close relationship to some PAH concentration reductions. PA showed excellent correlations with MMW and HMW (Pyr, BaA, CHR, BbF, BaP, and IND) PAHs, which may indicate that these PAHs partly decomposed into PA under the influence of plasma. Good correlations of PA with FL evinced the fact that recombination may also happen in a plasma atmosphere because

FL did not contain PA elements (as judged from its molecular structure) so the breakup into PA did not happen.

CONCLUSIONS

PAH emission concentrations of the diesel engine were high, and NTP technology showed excellent PAH removal performance. Based on the data presented in this paper, the following conclusions can be drawn:

(1) Total PAH concentration of the non-road diesel engine was 1,007.8 μg/m^3, 4,051.2 μg/m^3, and 2,173.5 μg/m^3 at 40%, 60%, and 80% engine load, respectively. The percentage of particle-phase components was 32.7%, 79.2%, and 55.0% respectively.

(2) The removal efficiency of total PAHs was 50.1%, 82.1%, and 65.2%, and it was more than 80% for particle-phase components at three different engine loads under the influence of NTP. PAH concentration ratios of particle- to gas-phase with NTP were almost the same (*c.* 0.13) at different engine loads under the influence of NTP.

(3) The most abundant compounds were among LMW and MMW PAHs at different engine loads. The Nap concentration increased under the effect of NTP due to the breakup of MMW and HMW PAHs in the plasma zone. The PAH content of PM aggregation at different loads was large.

(4) Excellent linearity was shown between the particle-phase and total PAH concentrations both with and without NTP. Gas-phase PAH concentrations linearly increased with engine load without NTP. Correlations of PAH concentrations and PAH concentration reduction formed a basis for an improved understanding of PAH formation and PAH reduction mechanisms with NTP technology.

ELECTRONIC SUPPLEMENTARY INFORMATION

Further information about the details of the limits of detection and recoveries, total PAH contents of PM aggregation, correlation values of PAHs, PAHs concentration reduction.

ACKNOWLEDGEMENTS

This work was supported by Science and Technology Planning Project of Hebei province, China (No. 15273703D). We gratefully acknowledge the Beijing Centre of Physical and Chemical Analysis for the PAH test of diesel engine exhaust.

SUPPORTING INFORMATION

Additional information as noted in the text. This information is available via the Internet at http://www.springer.com/chemistry/journal/11814.

REFERENCES

1. K. W. Jung, Y. J. Won, H. J. Kong, C. M. Oh, D. H. Lee and J. S. Lee, *Cancer Res. Treatment*, **46**(2), 109 (2014).
2. A. J. White, P. T. Bradshaw, A. H. Herring, S. L. Teitelbaum, J. Beyea, S. D. Stellman, S. E. Steck, I. Mordukhovich, S. M. Eng, L. S. Engel, K. Conway, M. Hatch, A. I. Neugut, R. M. Santella and M. D. Gammon, *Environ. Int.*, **89**, 185 (2016).
3. Y. S. Ge, C. He and X. K. Han, *Trans. CSICE*, **25**(2), 125 (2007).
4. F. Alkurdi, F. Karabet and M. Dimashki, *Atmospheric Res.*, **120**, 68 (2013).
5. V. Kumar and N. Kothiyal, *J. Environ. Res. Dev.*, **5**(3), 584 (2011).
6. M. Tavares, J. P. Pinto, A. L. Souza, I. S. Scarmínio and M. C. Solci, *Atmos. Environ.*, **38**(30), 5039 (2004).
7. M. C. Lim, G. A. Ayoko, L. Morawska, Z. D. Ristovski and E. R. Jayaratne, *Atmos. Environ.*, **39**(40), 7836 (2005).
8. C. He, Y. S. Ge, J. W. Tan, K. W. You, X. K. Han and J. F. Wang, *Fuel*, **89**(8), 2040 (2010).
9. S.-M. Chien, Y.-J. Huang, S.-C. Chuang and H.-H. Yang, *Aerosol Air Quality Res.*, **9**(1), 18 (2009).
10. G. Karavalakis, S. Stournas and E. Bakeas, *Atmos. Environ.*, **43**(10), 1745 (2009).
11. G. Karavalakisa, G. Deves, G. Fontaras, S. Stournas, Z. Samaras and E. Bakeas, *Fuel*, **89**(12), 3876 (2010).
12. G. Karavalakis, E. Bakeas and S. Stournas, *Environ. Sci. Technol.*, **44**(13), 5306 (2010).
13. Y. S. Mok and Y. J. Huh, *Plasma Chem. Plasma Process.*, **25**(6), 625 (2005).
14. B. Rajanikanth, D. Sinha and P. Emmanuel, *Plasma Sci. Technol.*, **10**(3), 307 (2008).
15. T. Vinh, S. Watanabe, T. Furuhata and M. Arai, *J. Energy Institute*, **85**(3), 163 (2012).
16. A. G. Chmielewski, Y. X. Sun, J. Licki, S. Bułka, K. Kubica and Z. Zimek, *RaPC*, **67**(3), 555 (2003).
17. The first construction machinery network, http://news.d1cm.com/2011/01/07/01071701229329.shtml.
18. F. Xu, Z. Y. Luo, P. Wang, Q. H. Hou, W. Cao, M. X. Fang and K. F. Cen, *Proceedings-Chinese Soc. Electrical Eng.*, **27**(32), 34 (2007).
19. M. Dong, Y. X. Cai, X. H. Li, F. Jiang and W. H. Han, *Applied Mechanics and Materials*, Trans Tech Publ, 1023.
20. Y. X. Cai, M. Dong, X. H. Li, F. Jiang and W. H. Han, *J. of Jiangsu University* (Natural Science Ed.), **35**(4), 380 (2014).
21. C. M. Du, J. H. Yan, X. D. Li, B. G. Cheron, X. F. You, Y. Chi, M. J. Ni and K. F. Cen, *PCPP*, **26**(5), 517 (2006).
22. L. Yu, X. Tu, X. D. Li, Y. Wang, Y. Chi and J. H. Yan, *J. Hazard. Mater.*, **180**(1), 449 (2010).
23. F. Portet-Koltalo and N. Machour, Analytical methodologies for the control of particle-phase polycyclic aromatic compounds from diesel engine exhaust. Diesel Engine Combustion, Emissions and Condition Monitoring Intech, ISBN. 978 (2013).
24. T. Lu, Z. Huang, C. S. Cheung and J. Ma, *Sci. Total Environ.*, **438**, 33 (2012).
25. R. De Abrantes, J. V. DE Assunção and C. R. Pesquero, *Atmos. Environ.*, **38**(11), 1631 (2004).
26. P. Spezzano, P. Picini and D. Cataldi, *Atmos. Environ.*, **43**(3), 539 (2009).
27. P. Spezzano, P. D. Cataldi, F. Messale and C. Manni, *Atmos. Environ.*, **42**(18), 4332 (2008).
28. G. Junhua, F. Maodong and Z. Zhongrong, *Trans. CSICE*, **5**, 423 (2009).
29. D. M. Lou, F. Gao, D. Yao, P. Q. Tan and Z. Y. Hu, *Trans. CICEE*,

35(4), 31 (2014).
30. W. P. Arnott, *Environ. Sci. Technol.*, **38**(9), 2557 (2004).
31. C. C. Ma, J. B. Gao, L. Zhong and S. K. Xing, *Appl. Therm. Eng.*, **99**, 1110 (2016).
32. S. K. Xing, C. C. Ma and S. Ma, *Chinese Internal Combustion Engine Engineering*, **1**, 8 (2013).
33. J.-O. Chae, *J. Electrostatics.*, **57**(3), 251 (2003).
34. R. G. Tonkyn, S. E. Barlow and J. W. Hoard, *Appl. Catal. B: Environ.*, **40**(3), 207 (2003).
35. C. L. Song, B. Feng, Z. M. Tao, F. C. Li and Q. F. Huang, *J. Hazard. Mater.*, **166**(1), 523 (2009).
36. P. M. Merritt, V. Ulmet, R. L. Mccormick, W. E. Mitchell and K. J. Baumgard, Regulated and unregulated exhaust emissions comparison for three tier II non-road diesel engines operating on ethanol-diesel blends: SAE Technical Paper; 2005. Report No.: 0148-7191.
37. T. Yamamoto, T. Mimura, N. Otsuka, Y. Ito, Y. Ehara and A. Zukeran, *IEEE Trans. Ind. Appl.*, **46**(4), 1606 (2010).
38. A. Zukeran, Y. Ikeda, Y. Ehara, M. Matsuyama, T. Ito, T. Takahashi, H. Kawakami and T. Takamatsu, *IEEE Trans. Ind. Appl.*, **35**(2), 346 (1999).
39. J.-B. Lee, J.-H. Hwang and B.-N. Bae, *JSME Int. J., Ser. B: Fluids and Thermal Engineering*, **43**(4), 602 (2000).
40. C. T. Pham, T. Kameda, A. Toriba and K. Hayakawa, *Environ. Pollut.*, **183**, 175 (2013).

Supporting Information

Polycyclic aromatic hydrocarbon emissions of non-road diesel engine treated with non-thermal plasma technology

Jianbing Gao*, Chaochen Ma*,†, Shikai Xing, Liwei Sun*, and Jiangquan Liu***

*School of Mechanical Engineering, Beijing Institute of Technology, Beijing 100081, China
**School of Vocational and Technical, Hebei Normal University, Shijiazhuang 050024, China
(*Received 22 May 2016 • accepted 1 August 2016*)

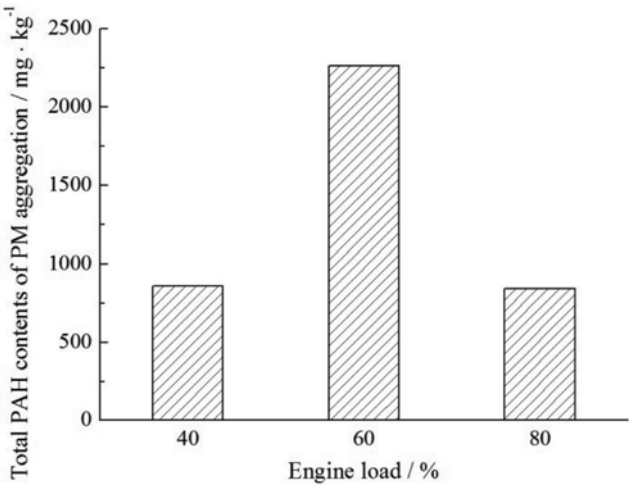

Fig. S1. Total PAH contents of PM aggregation.

Table S1. Limits of detection and recoveries of PAHs

	PAHs	Limit of detect/mg/L	Recoveries/ %	RSD/ %	Toxicity factors [1]
LMW	Nap	0.18	70.25	7.3	0.001
	Acp	0.03	103.46	2.5	0.001
	AcPy	0.03	100.12	6.1	0.001
	Flu	0.07	95.41	0.9	0.001
	PA	0.08	82.72	1.8	0.001
	Ant	0.12	85.93	3.4	0.01
MMW	FL	0.05	79.13	0.5	0.001
	Pyr	0.06	72.11	4.2	0.001
	BaA	0.31	69.94	0.7	0.1
	CHR	0.13	77.47	4.1	0.01
HMW	BbF	0.30	74.35	3.9	0.1
	BkF	0.16	80.13	10.1	0.1
	BaP	0.21	62.52	5.8	1
	IND	0.58	61.35	6.7	0.1
	DBA	0.67	55.78	2.7	1
	BghiP	0.27	58.92	3.4	0.01

Table S2. Correlation of PAHs without NTP

PAH	Nap	Acp	AcPy	Flu	PA	Ant	FL	Pyr	BaA	CHR	BbF	BkF	BaP	IND	DBA	BghiP	ΣPAHs
Nap	1.000																
Acp	0.991	1.000															
AcPy	0.949	0.898	1.000														
Flu	0.444	0.319	0.704	1.000													
PA	−0.282	−0.409	0.034	0.734	1.000												
Ant	−0.808	−0.880	−0.581	0.169	0.793	1.000											
FL	−0.137	−0.269	0.182	0.827	0.989	0.694	1.000										
Pyr	0.005	−0.130	0.320	0.898	0.958	0.585	0.990	1.000									
BaA	−0.017	−0.151	0.299	0.889	0.964	0.603	0.993	1.000	1.000								
CHR	0.125	−0.010	0.431	0.945	0.916	0.484	0.966	0.993	0.990	1.000							
BbF	0.328	0.197	0.608	0.992	0.814	0.292	0.891	0.946	0.939	0.978	1.000						
BkF	0.275	0.402	−0.042	−0.740	−1.000	−0.789	−0.990	−0.960	−0.966	−0.920	−0.818	1.000					
BaP	−0.406	−0.526	−0.098	0.638	0.991	0.867	0.961	0.912	0.920	0.856	0.730	−0.990	1.000				
IND	−0.143	−0.275	0.176	0.824	0.990	0.698	1.000	0.989	0.992	0.964	0.888	−0.991	0.962	1.000			
DBA	0.939	0.884	1.000	0.724	0.064	−0.557	0.211	0.348	0.328	0.458	0.632	−0.072	−0.068	0.206	1.000		
BghiP	−0.552	−0.435	−0.787	−0.992	−0.644	−0.045	−0.751	−0.837	−0.825	−0.896	−0.969	0.650	−0.538	−0.747	−0.805	1.000	
ΣPAHs	0.093	−0.042	0.402	0.934	0.929	0.511	0.974	0.996	0.994	0.999	0.971	−0.932	0.872	0.972	0.429	−0.882	1.000

Table S3. Correlation of PAH concentration reduction

	Nap	Acp	AcPy	Flu	PA	Ant	FL	Pyr	BaA	CHR	BbF	BkF	BaP	IND	DBA	BghiP	ΣPAHs
Nap	1.000																
Acp	0.968	1.000															
AcPy	0.778	0.594	1.000														
Flu	0.720	0.872	0.124	1.000													
PA	0.237	0.475	–0.425	0.845	1.000												
Ant	–0.335	–0.087	–0.853	0.413	0.836	1.000											
FL	0.372	0.595	–0.293	0.912	0.990	0.750	1.000										
Pyr	0.330	0.557	–0.337	0.893	0.995	0.779	0.999	1.000									
BaA	0.359	0.583	–0.307	0.906	0.992	0.759	1.000	1.000	1.000								
CHR	0.447	0.658	–0.214	0.943	0.975	0.693	0.997	0.992	0.995	1.000							
BbF	0.484	0.690	–0.172	0.956	0.965	0.662	0.992	0.986	0.990	0.999	1.000						
BkF	–0.120	–0.367	0.530	–0.776	–0.993	–0.895	–0.966	–0.977	–0.970	–0.942	–0.927	1.000					
BaP	–0.032	0.221	–0.653	0.671	0.963	0.952	0.916	0.933	0.921	0.880	0.859	–0.988	1.000				
IND	0.197	0.438	–0.463	0.822	0.999	0.858	0.983	0.991	0.986	0.965	0.953	–0.997	0.974	1.000			
DBA	0.996	0.942	0.830	0.657	0.152	–0.416	0.290	0.246	0.277	0.367	0.406	–0.033	–0.119	0.111	1.000		
BghiP	–0.932	–0.993	–0.497	–0.923	–0.574	–0.029	–0.684	–0.650	–0.674	–0.741	–0.769	0.472	–0.333	–0.539	–0.897	1.000	
ΣPAHs	0.386	0.606	–0.279	0.918	0.988	0.740	1.000	0.998	1.000	0.998	0.994	–0.962	0.910	0.980	0.304	–0.694	1.000

1. I. C. Nisbet and P. K. LaGoy, *Regulatory Toxicology and Pharmacology*, **16**(3), 290 (1992).